NACA RM E50L28

FOR REFERENCE
NOT TO BE TAKEN FROM THIS ROOM
FEB 19 1951
N-4784
c. 1

NACA

RESEARCH MEMORANDUM

TENSILE-FRACTURING CHARACTERISTICS OF SEVERAL HIGH-TEMPERATURE ALLOYS AS INFLUENCED BY ORIENTATION IN RESPECT TO FORGING DIRECTION

By W. F. Brown, Jr., H. Schwartzbart, and M. H. Jones

Lewis Flight Propulsion Laboratory
Cleveland, Ohio

NATIONAL ADVISORY COMMITTEE
FOR AERONAUTICS

WASHINGTON
February 12, 1951

NACA LIBRARY
LANGLEY AERONAUTICAL LABORATORY

NASA Library
3 1176 01435 2141

1

NATIONAL ADVISORY COMMITTEE FOR AERONAUTICS

RESEARCH MEMORANDUM

2023

TENSILE-FRACTURING CHARACTERISTICS OF SEVERAL HIGH-TEMPERATURE ALLOYS AS INFLUENCED BY ORIENTATION IN RESPECT TO FORGING DIRECTION

By W. F. Brown, Jr., H. Schwartzbart, and M. H. Jones

SUMMARY

The effects of specimen-axis orientation with respect to forging direction on the true stress-strain curves and the fracturing characteristics at room temperature of forged and subsequently heat-treated billets of alloys 16-25-6, S-816, and Inconel X were investigated.

Forging of these alloys produced a mechanical anisotropy of fracture properties that was pronounced for 16-25-6, somewhat less for S-816, and slight for Inconel X. In the case of 16-25-6, the ductilities of specimens having orientations greater than 60° were less than one-half the value of a specimen having an orientation of 0° (axis parallel to forging direction). The stress producing a given plastic strain below the fracture strain was only slightly affected, however, by the specimen orientation.

Comparison among data of the three investigated alloys and data of several other materials obtained from reference reports indicated that mechanical anisotropy affected the fracturing characteristics of all the materials in the same general manner.

INTRODUCTION

Hot or cold deformation of metals can produce anisotropy, or directionality, of the mechanical properties. This anisotropy is of two main types: crystallographic anisotropy due to preferred orientation of the metal crystals and mechanical anisotropy due to orientation and elongation of inclusions, cavities, and precipitates that occur during hot working and that produce a fibrous structure.

As shown by Unckel (reference 1), Klingler and Sachs (reference 2), Baldwin, Howald, and Ross (reference 3), Phillips and Dunkle (reference 4), and others, crystallographic anisotropy

results from cold working and may be present after annealing if the cold deformations are severe. This process causes continuous variations in the stress-strain and fracture properties with the direction of testing. The magnitude of these effects depend on the past working and thermal history of the alloy and can be explained by considering the plastic anisotropy of the individual grains.

2023

Mechanical anisotropy or fibering primarily results from hot working (reference 5) and in some cases is difficult to remove by any reasonable heat treatment, as shown in reference 6. This type of anisotropy is considered to be the probable cause of lower transverse ductility and impact strength of many steel and aluminum forgings. The transverse ductility may thus be less than one-half the value in the forging direction. The manner in which fibering influences the variation of plastic and fracture properties is not definitely known.

Scattered information is available on the variation of ductility with testing direction resulting from both types of anisotropy for several different metals (references 1, 2, 4, 5, and 7). Only reference 7, however, reports associate changes in the fracture stress and none of the references attempts to correlate directly the variations in mechanical properties with the microstructure. The evidence presented thus far indicates that fibering certainly has little or no effect on the plastic properties but may have a pronounced effect on the fracture characteristics.

Turbine components, such as blades, blade fastenings, and wheels, undergo plastic flow during service and the life of such components may be influenced by either one or both of the anisotropies previously mentioned. The optimum design of these components having complicated contours would require a knowledge of the stress-strain and fracture characteristics and how they are influenced by the direction of stressing as related to the principal deformation direction in previous working. In such cases, it would be advantageous to have the axis of the algebraically smallest stress coincide with the weakest metal direction. Conversely, if the conditions of test or service are not severely embrittling, the fracture stress is insignificant to the designer and a condition of instability or some small limiting strain may determine failure. In such cases, the conventional yield, tensile, creep, or rupture strengths (all based on the initial area) are used as a basis for design.

In order to study the mechanical anisotropy in typical high-temperature alloys, an investigation was conducted at the NACA Lewis laboratory and is presented herein. The influence of the

2023

testing direction in relation to the forging direction on the true stress-strain curves and fracture characteristics was determined for S-816, Inconel X, and 16-25-6 alloys. These alloys were chosen as representatives of cobalt-nickel-chromium, nickel, and iron base alloys, respectively. Forgings with approximately 4-inch diameters were selected to approach the conditions encountered in commercial fabrication. In order to represent a problem as fundamental and simple as possible and to permit comparison with data on other metals obtained from reference reports, the alloys were worked in one direction only.

Tensile tests at room temperature were considered most suitable for a preliminary investigation because these metals, which do not neck deeply, are subjected to a simple state of stress and thus offer the maximum opportunity for any mathematical analysis. Orientation angles from 0° to 90° (between the forging direction and the specimen axis) were investigated. Data obtained from the investigation reported herein are compared with data obtained from reference reports and an attempt is made to correlate the observed changes with microstructures of the forgings.

MATERIAL AND SPECIMEN PREPARATION

The nominal compositions, as furnished by the suppliers, and the average Rockwell-C hardnesses of cross sections of the three alloys investigated are shown in the following table:

Alloy	Cr	Co	Ni	Mo	C	Fe	Mn	N	W	Cb	Si	Ti	Al	Rockwell-C hardness
16-25-6	16.4	--	25.2	5.8	0.08	bal.	1.6	0.164	----	----	0.68	----	----	26±2
S-816	19.8	43	20.4	4.3	.38	2.8	1.53	-----	4.05	3.51	.26	----	----	26±2
Inconel X	14.56	--	73.10	---	.04	7.01	.53	-----	----	.98	.44	2.38	0.90	22±3

Attempts were made to obtain forgings of known working history. The Inconel X alloy was: (1) forged at 2225° F from an 18-inch square ingot to a $12\frac{1}{4}$-inch octagon and air-cooled; (2) forged to a 6-inch square at 2225° F and air-cooled; (3) rolled to $4\frac{1}{2}$-inch diameter at 2200° F and quenched; and (4) machined to a 4-inch diameter. The 16-25-6 alloy was: (1) hot-forged at 2100° F from

an ingot of unknown size to a $4\frac{3}{8}$-inch square; and (2) hot-cold worked at 1200° F to a 4-inch octagon (approximately 22-percent reduction). The S-816 alloy was: (1) forged at 2250° F from a 9-inch diameter ingot to a 6-inch square; (2) forged at 2200° F to a 4-inch square; and (3) solution-treated at 2250° F and water-quenched, followed by aging at 1400° F for 6 hours and air-cooling. 2023

Sections 4 inches long were cut from the ends of the forged bars and a plate approximately 4 inches wide containing the bar axis was cut from each section (fig. 1). The angular position of the plate in relation to any specific bar diameter was unimportant because macroetching revealed the structure of the forgings to be uniform over the cross sections. A hardness survey of the bar cross sections showed the Rockwell-C hardness to be uniform within ±3 points. Specimen blanks were then cut from the plates at the location shown in figure 1. In order to insure that any radial nonuniformity of working, which may be present, did not influence the results, all specimen centers were taken at the same distance from the bar axis.

Buttonhead specimens of the type shown in figure 2 were rough machined from the blanks without the 2.7-inch radius. The rough-machined specimens were heat-treated according to the following conditions:

Alloy	Solution temperature (°F)	Solution time (hr)	Aging temperature (°F)	Aging time (hr)
16-25-6	----	-	1200	4
S-816	2300	1	1400	16
Inconel X	2100	4	1550 1300	24 20

The S-816 alloy was air-cooled and Inconel X was oil-quenched from the solution temperatures; all alloys were air-cooled from the aging temperatures. The specimens were finished by grinding, with particular care being taken to maintain concentricity of the cylindrical sections and to insure that the areas under the buttonheads were square with the specimen axis. The cross sections of the specimens were tapered to a minimum diameter at the center by grinding a 2.7-inch radius, as shown in figure 2. This radius is sufficiently large so that its effects on the stress state can be neglected (fig. 19 of reference 8). A reduced cross section at the center

2023

was necessary for two reasons: (1) because fracture would definitely take place at the strain-measuring location, and (2) because maximum stress would be restricted to a given location with respect to the geometry of the original forged bar.

A number was stamped on the end of each specimen for identification as to orientation. Specimen orientation is defined by the angle between the specimen axis and the forging direction, which is assumed to coincide with the bar axis, as shown in figure 1. An orientation angle of 0° thus describes a specimen the axis of which was originally parallel to the forging direction of the forged bars; whereas one of 90° describes a specimen the axis of which was originally radial with respect to the bar (transverse direction).

APPARATUS AND PROCEDURE

The tensile investigations were made with a hydraulic tensile machine. Specimens were fractured in a special concentric loading fixture (fig. 3), which is similar to a design described in reference 9. This fixture insures that the load is initially applied coincident (within 0.0005 in.) with the specimen axis in order to eliminate bending moments.

Reduction in diameter at the minimum cross section during loading was measured by means of a mechanical radial strain gage (fig. 4) and was mounted on the specimen as shown in figure 3. With this method, diameter changes of 0.00005 inch could be determined over a total range of 0.024 inch. This range corresponds to a minimum longitudinal strain of 0.00048 and a maximum longitudinal natural strain of 0.24 for this size specimen. Measurements with the gage were made up to a change in diameter of 0.020 inch and if fracture had not occurred, measurements were continued with point micrometers. In order to determine the final diameter, the two halves of the broken specimen were matched and the minimum cross section was measured on several different diameters with point micrometers.

Photographs at magnifications of 8 and 250 were prepared for fractured specimens representing selected orientations. In each case, the plane of the photograph is parallel to the forging direction and contains the specimen axis.

RESULTS AND DISCUSSION

The tensile data are assembled in the form of true stress - strain curves in figure 5. Each part of the figure represents one alloy and shows data for orientations of 0°, 30°, 60°, and 90°; these values adequately cover the range investigated. The natural longitudinal strain δ (reference 10) was calculated from the equation: 2023

$$\delta = 2 \log_e \frac{d_o}{d}$$

or

$$\delta = 2 \log_e \frac{d_o}{d_o - \Delta g}$$

where d_o is the initial diameter of the minimum cross section, d is the diameter at any load, and Δg is the change in diameter as determined by the gage reading. The value so calculated is equal to the natural longitudinal strain in the plastic region assuming constant volume and does not represent the longitudinal strain in the elastic region or where Poisson's ratio is not equal to 0.5.

The tensile properties of the various specimens are summarized in figure 6 as a function of orientation. The yield strength was determined at 0.2-percent plastic strain. This yield strength is not identical with the value that would be obtained from calculations based on longitudinal strain but is slightly higher. This difference depends on the unknown variation of Poisson's ratio in going from the elastic to the plastic range. The fracture stress was obtained by extrapolation of the stress-strain curves to a strain equal to the ductility or the natural longitudinal strain at fracture.

Plastic Properties

In figure 5, the stress at a given strain is shown to be nearly independent of specimen orientation for all three alloys. Hot-cold working of 16-25-6 alloy that affected approximately 22-percent reduction in area has therefore not produced a noticeable crystallographic anisotropy. The isotropy of plastic strain is further indicated by the diameter measurements on the fractured specimens, which show all specimens to have retained a circular cross section to fracture.

The strain-hardening rate of 16-25-6 is considerably lower than that of S-816 or Inconel X. This difference is also shown in the necking strain, which is 0.18 for 16-25-6 as compared with 0.26 for Inconel X; S-816 fractured before necking. These necking strains were determined by graphical differentiation of the stress-strain curves to yield the stress at necking, according to the following relation given by Sachs (reference 11) and others for slope at this point:

2023

$$\frac{d\sigma}{d\delta} = \sigma$$

where σ is the true stress and δ is the natural longitudinal strain.

The yield strength is independent of specimen orientation (fig. 6) as would be expected from the identity of the true stress - strain curves. Tensile strength would also be independent of the orientation except in cases where the ductility is less than the necking strain. This fact accounts for the slightly lower tensile strengths of specimens of 16-25-6 and S-816 having orientation angles greater than 60°.

Fracture Properties

Fracture stress and ductility of the three alloys investigated are influenced by specimen orientation (fig. 6). The curves for the three materials have the same general shape; the fracture characteristics are practically constant for orientations less than approximately 40° and constant at a lower value for orientations greater than approximately 60°. The change in values is pronounced for 16-25-6, somewhat less for S-816, and small for Inconel X. In figure 6, 16-25-6 and S-816 show a loss in ductility of approximately 60 and 30 percent, respectively, when orientations greater than 60° are compared with 0°. The corresponding decreases in fracture stresses are, however, approximately 19 and 14 percent. This smaller effect of ductility on the fracture stress for 16-25-6 is explained by its lower strain-hardening rate.

Examination of etched longitudinal specimen sections having orientations of 0° and 90° at a magnification of 8 (fig. 7) show a fibering of all three alloys parallel to the forging direction. The fibering is most pronounced for 16-25-6 and barely distinguishable for Inconel X and S-816. Photographs of the longitudinal sections near the specimen axis of 16-25-6 are shown at a magnification of 8 in figures 7 and 8 and at a magnification of 250 in

figure 9 for orientations of 0°, 45°, 60°, 75°, and 90°. These figures indicate that fibering in 16-25-6 is associated with formation of a precipitate in definite layers throughout the structure. Such a structure has been reported by Fleischmann (reference 12) for this alloy after various aging treatments but is absent in the solution-quenched condition. In addition, Freeman, Reynolds, and White (reference 13) have shown this layered precipitate to be present in commercial disk forgings. For orientations greater than 60°, the fracture apparently follows the precipitate planes, whereas for small orientation angles, the fracture surface is perpendicular to the specimen axis (fig. 9). It is interesting to note that plastic flow, which occurred during tensile straining in the 45° specimen (fig. 8(a)), produced a noticeable decrease in the angle between the fiber plane and the specimen axis.

2023

True stress - strain curves and yield strengths of the alloys investigated were insignificantly affected by differences in the direction of stressing in relation to the forging direction. The hot working has produced, however, a mechanical anisotropy that influenced the fracture characteristics of all the alloys in the same general manner. Thus, where weakness can be measured by fracturing characteristics, the forging direction should probably be considered in the design of parts in which the principal tensile stress is applied at an angle greater than 30°.

In figure 10, the results from this investigation are compared with data for several rolled and forged materials obtained from references 1, 6, and 7. In most of the reference data, fracture stresses were not reported and the comparison is made on the basis of ductility or fracture strain. Although the reference investigations did not include metallographic examination of the specimens, all the materials were worked in such a manner that they might be expected to possess a fibrous structure. Each material except the pure copper was solution heat-treated. The SAE 1045 and SAE 4334 steels possessed 0.1-percent yield strengths of 130,000 and 146,000 pounds per square inch, respectively. All the curves have the same general shape with the indication that orientations above approximately 60° are characterized by constant and low values of ductility.

A possible explanation for the variation in mechanical properties could be given if the precipitated material producing the fibrous structure were considered as constituting planes of weakness. The location of fracture would then follow the weakness planes when a certain stress condition is reached on these planes.

2023

The simplest assumption would be that fracture occurs on a weakness plane when the resolved normal stress on this plane exceeds the fracture stress of the 90° specimen, which is assumed to yield the true fracture stress of the weak material. The variation of fracture stress with specimen orientation can be determined by using this concept. Thus, the stress σ_n normal to a plane of weakness inclined at an angle θ (the previously defined orientation angle) to the specimen axis would be given in terms of the applied longitudinal stress σ_l as

$$\sigma_n = \sigma_l \sin^2 \theta$$

The minimum angle at which fracture is hypothesized to occur on the weakness plane θ_f can be determined if the fracture stress of the 90° specimen $\sigma_{n,f}$ and the fracture stress of the 0° specimen $\sigma_{l,f}$ are substituted for σ_n and σ_l, respectively, in the preceding equation. For angles equal to or greater than this value, fracture should occur along the weakness plane and the observed fracture stress σ_f should decrease according to the following function:

$$\sigma_f = \frac{\sigma_{n,f}}{\sin^2 \theta}$$

Fracture stresses for 16-25-6, S-816, and Inconel X specimens of various orientations were computed on the basis of this simple theory and are compared with those actually observed in figure 11. In each case there is poor agreement between the calculated and experimental values. A more detailed analysis of the problem and consideration of the effects of both the shear and normal stress on the weakness plane are apparently necessary.

SUMMARY OF RESULTS

An investigation was conducted to determine the effects of variation in the angle between the specimen axis and the forging direction on the tensile, plastic, and fracture characteristics at room temperature for alloys 16-25-6, Inconel X, and S-816. The following results were obtained:

1. Fracturing characteristics of the three alloys investigated exhibited an anisotropy that was pronounced for 16-25-6, somewhat less for S-816, and small for Inconel X. Ductilities of

16-25-6 specimens having orientations greater than 60° were less than one-half of the value in the forging direction.

2. The anisotropy of 16-25-6 was associated with planes of precipitate that were parallel to the forging direction in the original bar and that constituted the fracture plane of specimens at orientations greater than 60°. 2023

3. For the three alloys considered in this investigation, the fracture stress and the ductility decreased rapidly in the range of orientations from 40° to 60° and then remained constant to 90°.

4. A comparison of the results obtained in this investigation with data from reference reports for several other materials indicated that, in general, materials that exhibited mechanical fibering had fracture properties that decreased to a constant value at orientations greater than approximately 60°.

5. The identity of true stress - strain curves for specimens of various orientations and the fact that the specimens were circular in cross section at fracture indicated that the alloys were essentially crystallographically isotropic.

Lewis Flight Propulsion Laboratory,
National Advisory Committee for Aeronautics,
Cleveland, Ohio.

REFERENCES

1. Unckel, Hermann: Die mechanischen Eigenschaften kaltgewordener Werkstoffe in Abhängigkeit von Walzgrad, Korngrösse und Probenrichtung. Zeitschr. f. Metallkunde, Jahrg. 31, Heft 4, April 1939, S. 104-108.

2. Klingler, L. J., and Sachs, G.: Plastic Flow Characteristics of Aluminum-Alloy Plate. Jour. Aero. Sci., vol. 15, no. 10, Oct. 1948, pp. 599-604.

3. Baldwin, William M., Jr., Howald, T. S., and Ross, A. W.: Relative Triaxial Deformation Rates. Metals Tech., vol. 12, no. 6, Sept. 1945, pp. 13-24.

4. Phillips, Arthur, and Dunkle, H. H.: Directional Properties in Rolled and Annealed Low Carbon Steel. Trans. A.S.M., vol. 23, June 1934, pp. 398-405; discussion, pp. 405-408.

2023

5. Sachs, George: Some Observations on the Forging of Strong Aluminum Alloys. Jour. Inst. Metals, vol. 6, pt. 1, Jan. 1939, pp. 9-31.

6. Wells, Cyril, and Mehl, Robert F.: Transverse Mechanical Properties in Heat Treated Wrought Steel Products. Trans. A.S.M., vol. 41, 1949, pp. 715-805; discussion, pp. 806-818.

7. Klingler, L. J., and Sachs, G.: Fracturing Characteristics of Aluminum-Alloy Plate. Jour. Aero. Sci., vol. 15, no. 12, Dec. 1948, pp. 731-734.

8. Dana, A. W., Aul, E. L., and Sachs, G.: Tension Properties of Aluminum Alloys in the Presence of Stress-Raisers. I - Effects of Triaxial Stress States on the Fracturing Characteristics of 24S-T Aluminum Alloy. NACA TN 1830, 1949.

9. Sachs, G., Lubahn, J. D., and Ebert, L. J.: Notched Bar Tensile Test Characteristics of Heat Treated Low Alloy Steels. Trans. A.S.M., vol. 33, 1944, pp. 340-391.

10. Sachs, George, and Van Horn, Kent R.: Practical Metallurgy. Am. Soc. Metals (Cleveland), 1940.

11. Sachs, G., and Lubahn, J. D.: Failure of Ductile Metals in Tension. Trans. A.S.M.E., vol. 68, no. 4, May 1946, pp. 271-276.

12. Fleischmann, Martin: 16-25-6 Alloy for Gas Turbines. Iron Age, vol. 157, no. 3, Jan. 17, 1946, pp. 44-53; cont., vol. 157, no. 4, Jan. 24, 1946, pp. 50-60.

13. Freeman, J. W., Reynolds, E. E., and White, A. E.: A Metallurgical Investigation of Five Forged Gas-Turbine Discs of Timken Alloy. NACA TN 1531, 1948.

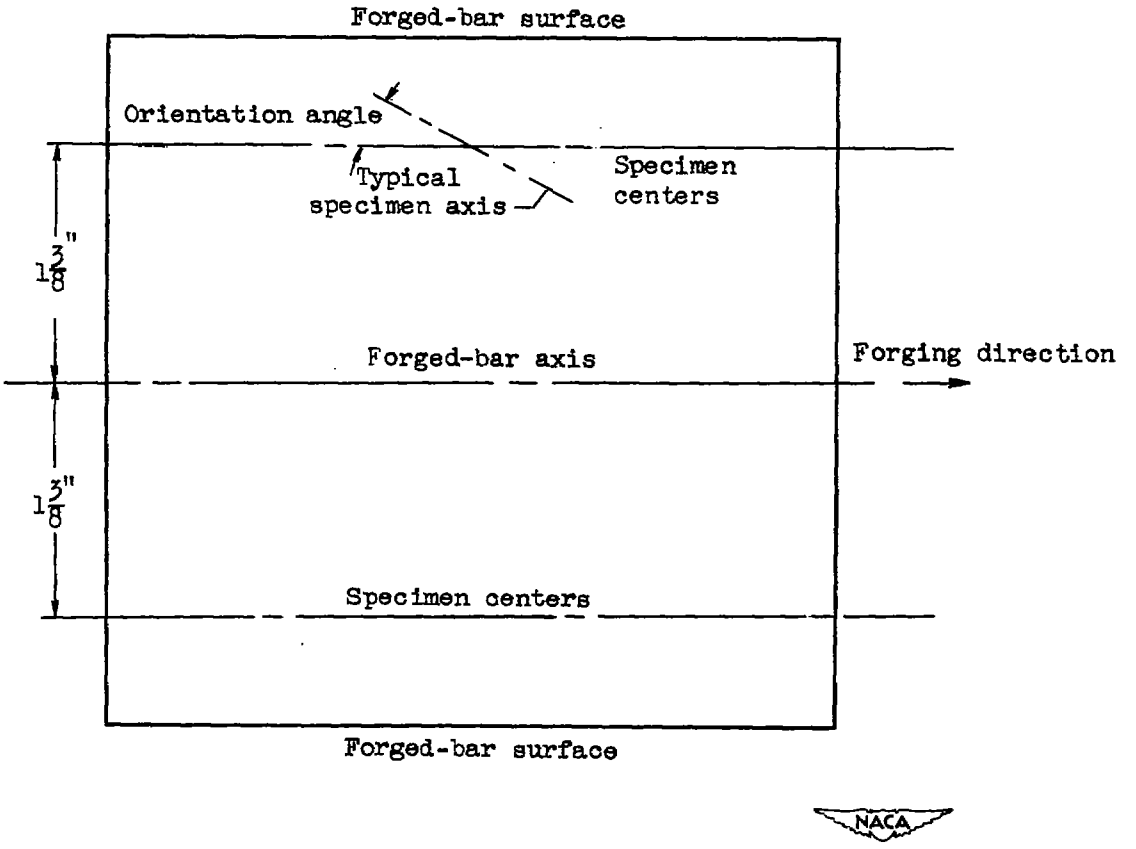

Figure 1. - Location of specimen centers in plate cut from forged bars and angular relation between forging direction and specimen axis.

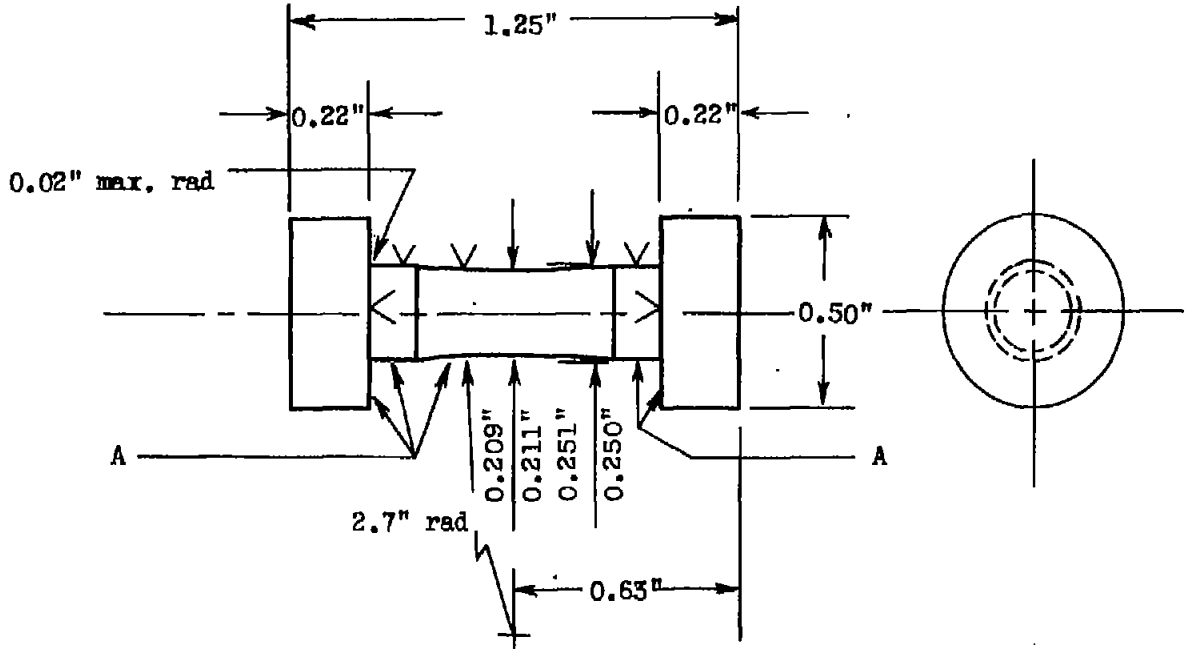

A Surfaces must be flat, square, and concentric to within 0.0005 total indicator reading. Finished surfaces must be 16 microinches rms.

Figure 2. - Buttonhead tensile specimen.

2023

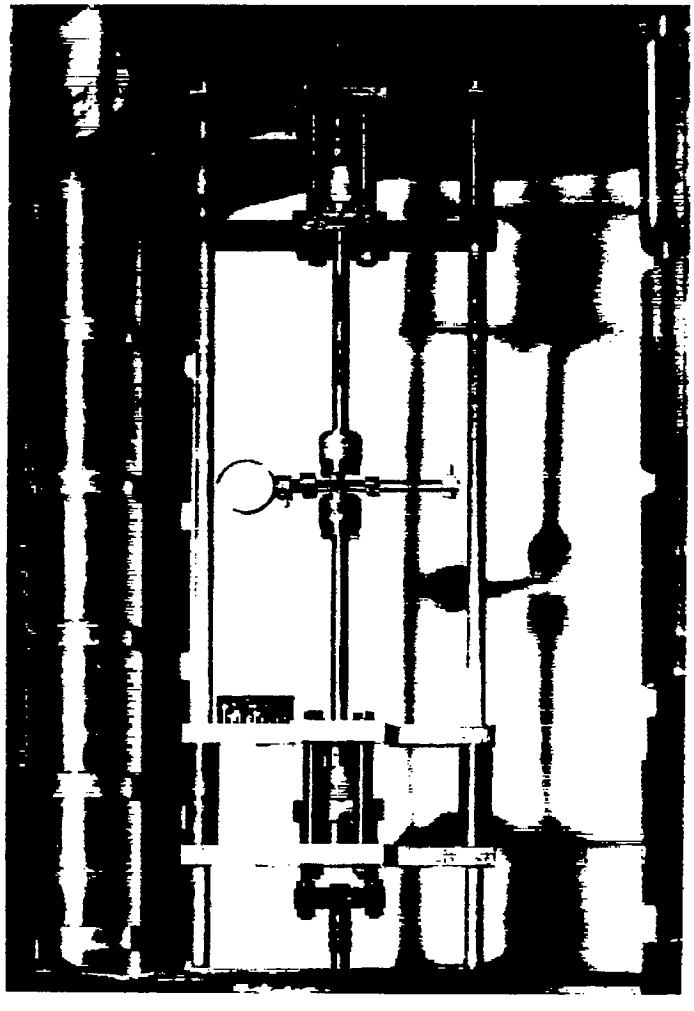

C-23834

Figure 3. - Concentric tensile loading fixture with radial strain gage mounted on specimen.

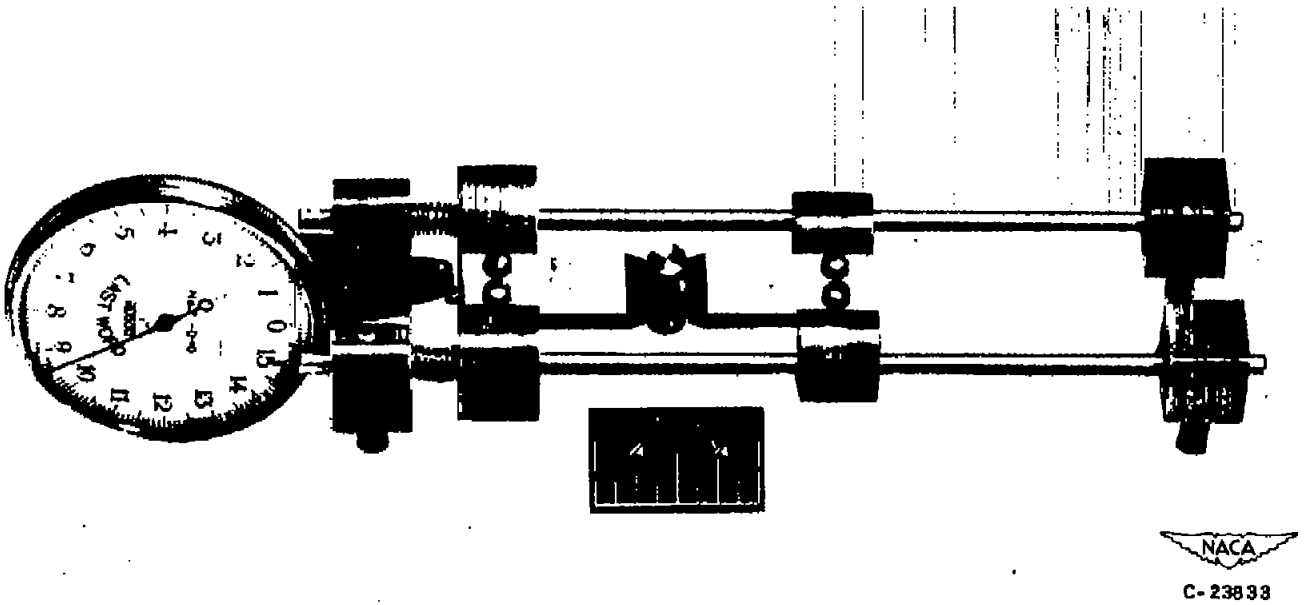

Figure 4. - Radial strain gage for measuring diameter changes.

2023

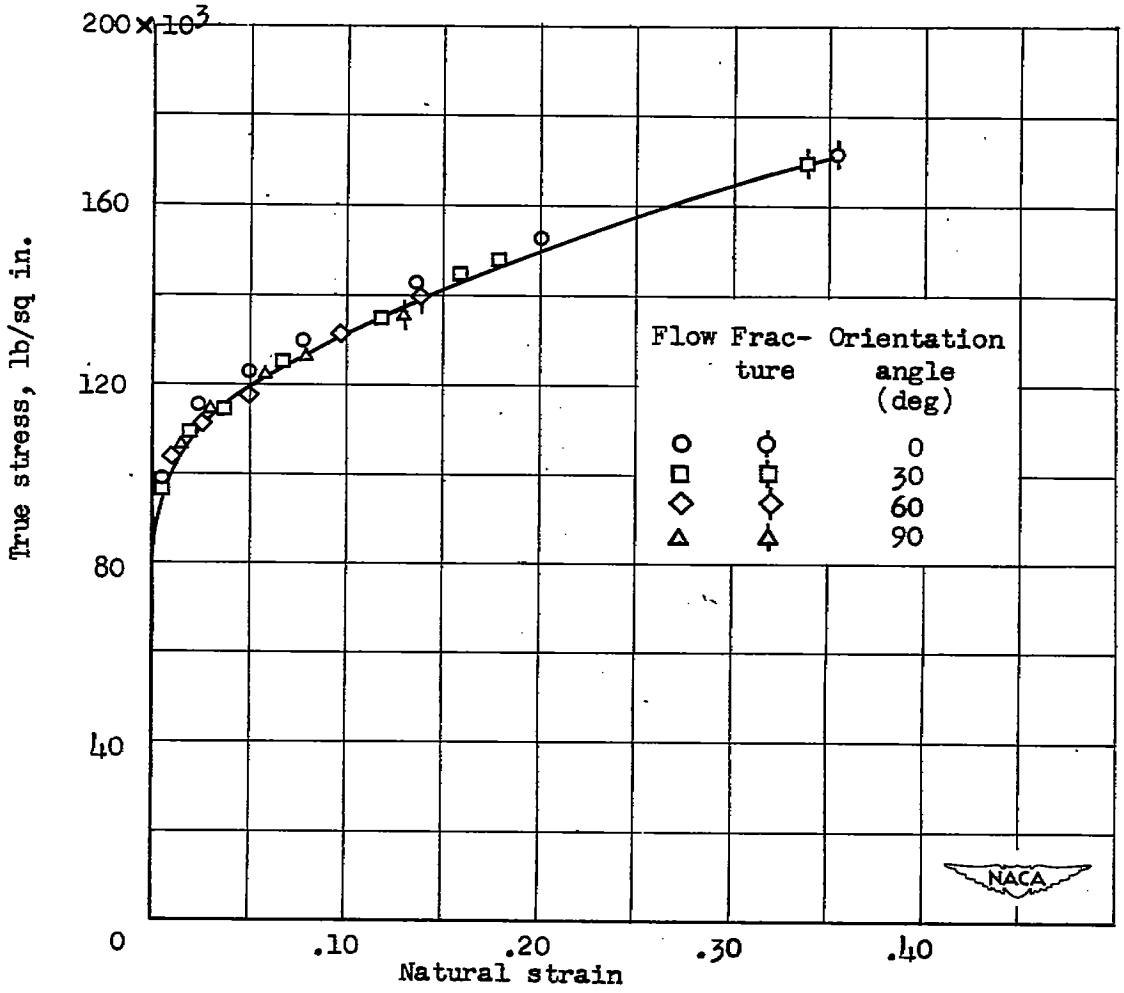

(a) Hot-cold worked and aged 16-25-6.

Figure 5. - Stress-strain curves for various orientations of three alloys.

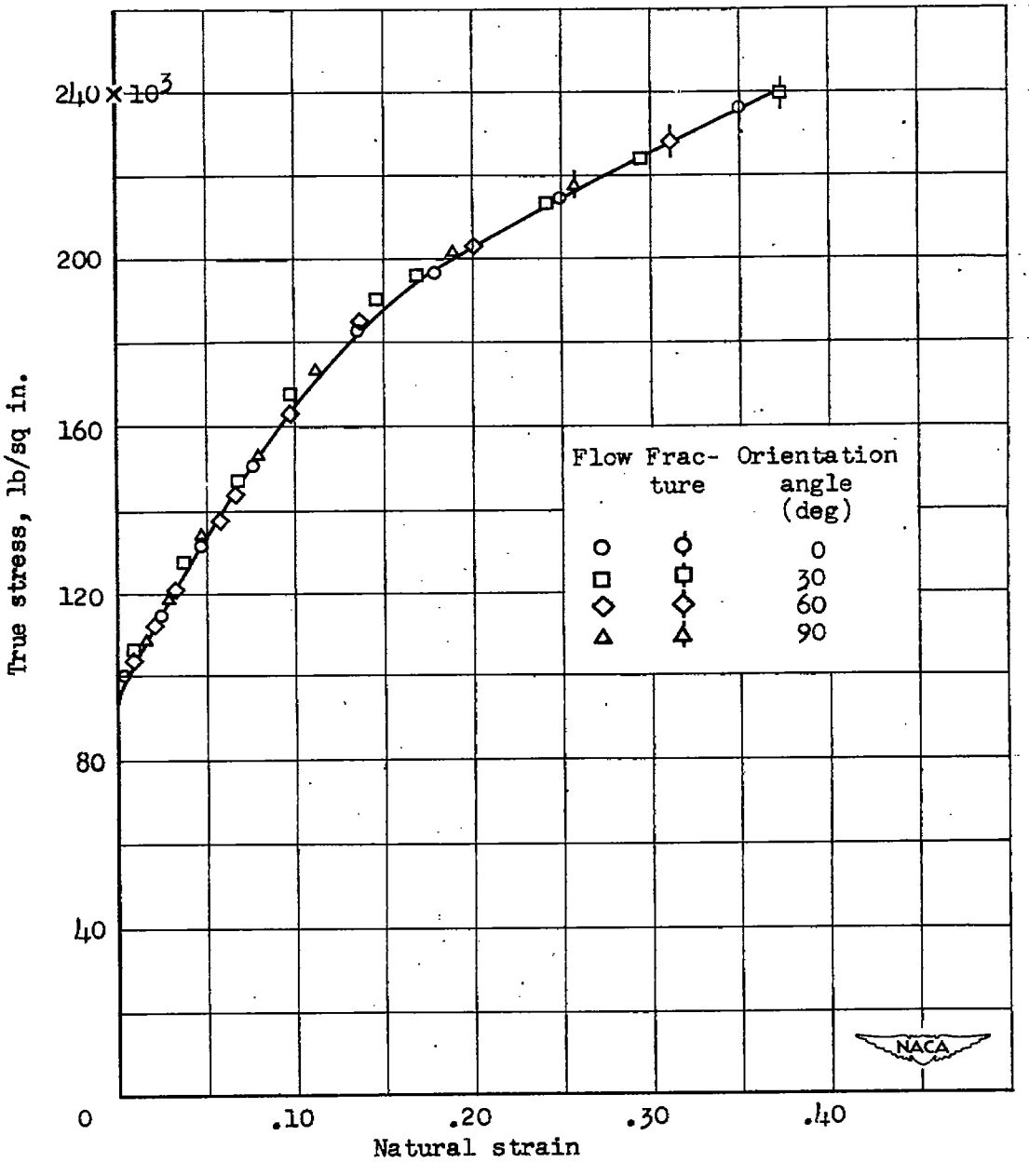

(b) Forged and heat-treated Inconel X.

Figure 5. - Continued. Stress-strain curves for various orientations of three alloys.

2023

2023

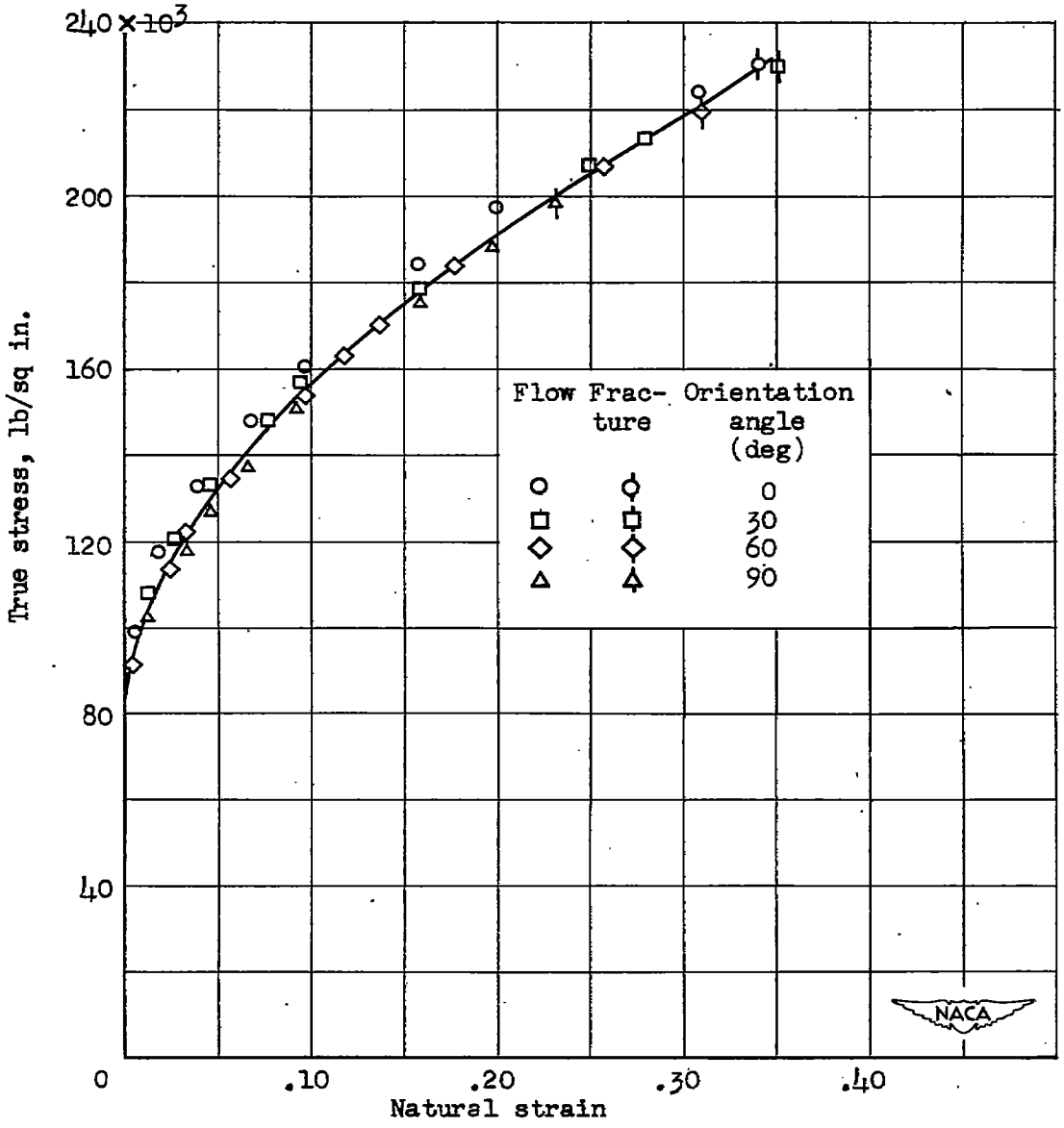

(c) Forged and heat-treated S-816.

Figure 5. - Concluded. Stress-strain curves for various orientations of three alloys.

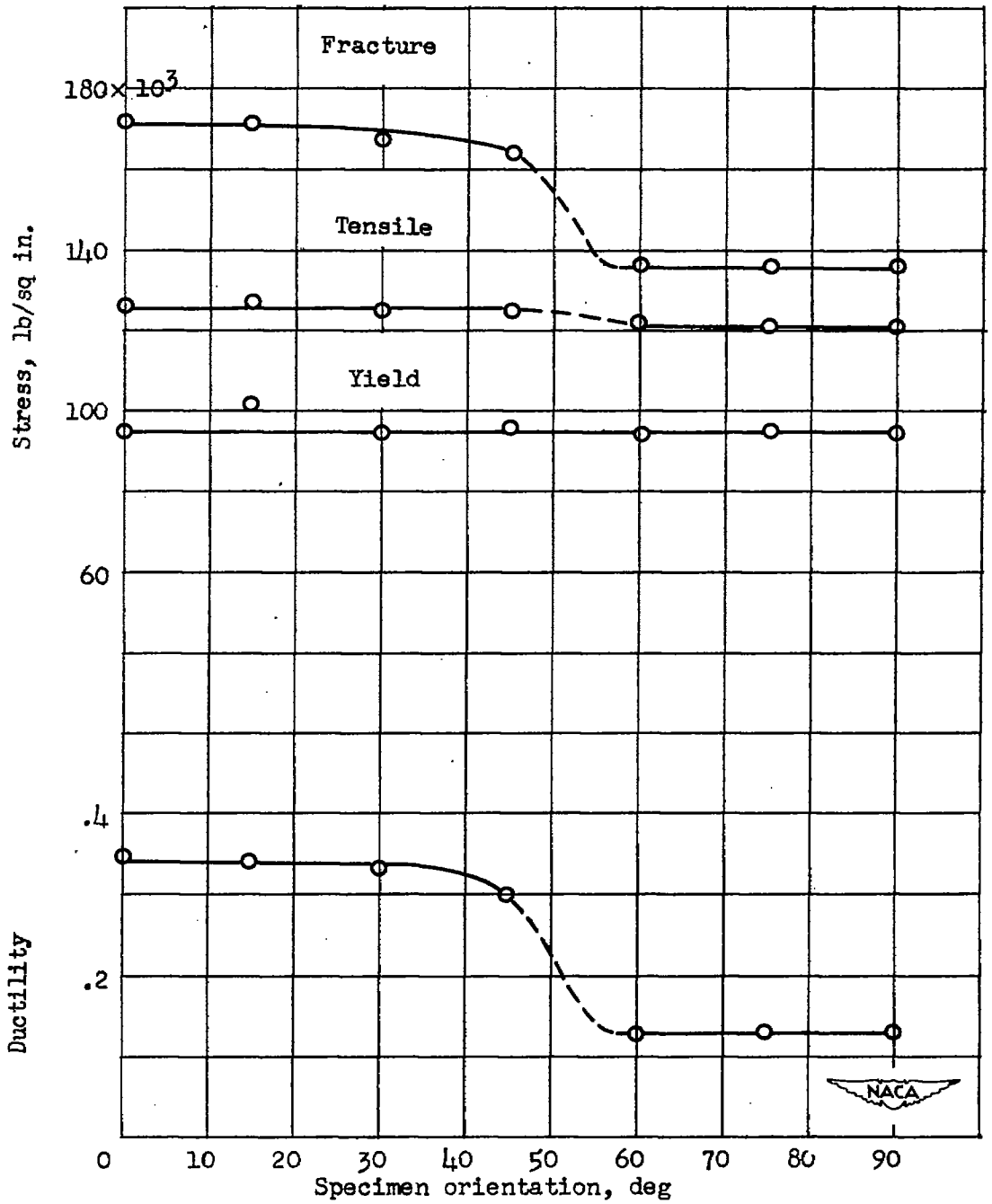

(a) Hot-cold worked and aged 16-25-6.

Figure 6. - Variation of tensile properties with testing direction of three alloys.

2023

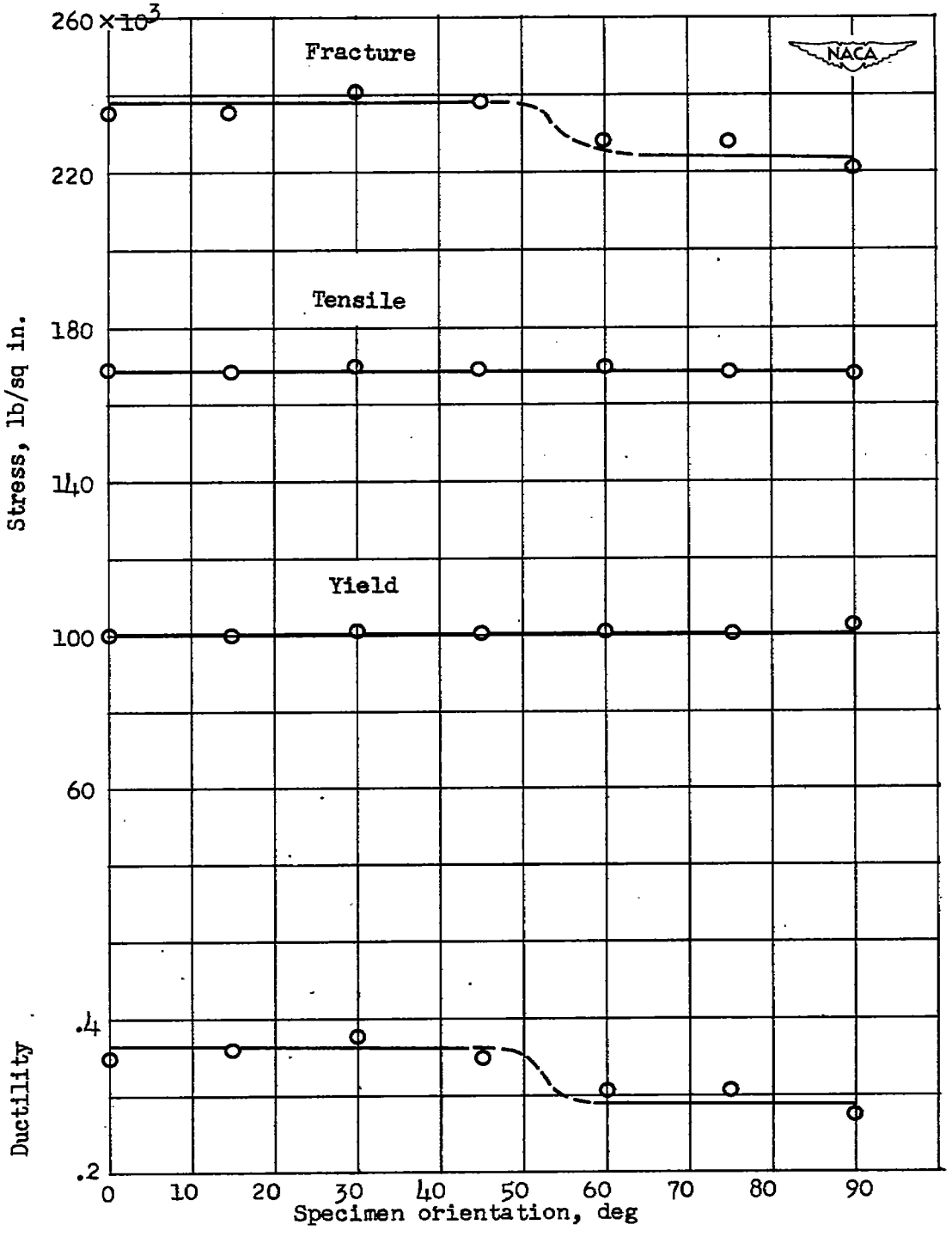

(b) Forged and heat-treated Inconel X.

Figure 6. - Continued. Variation of tensile properties with testing direction of several alloys.

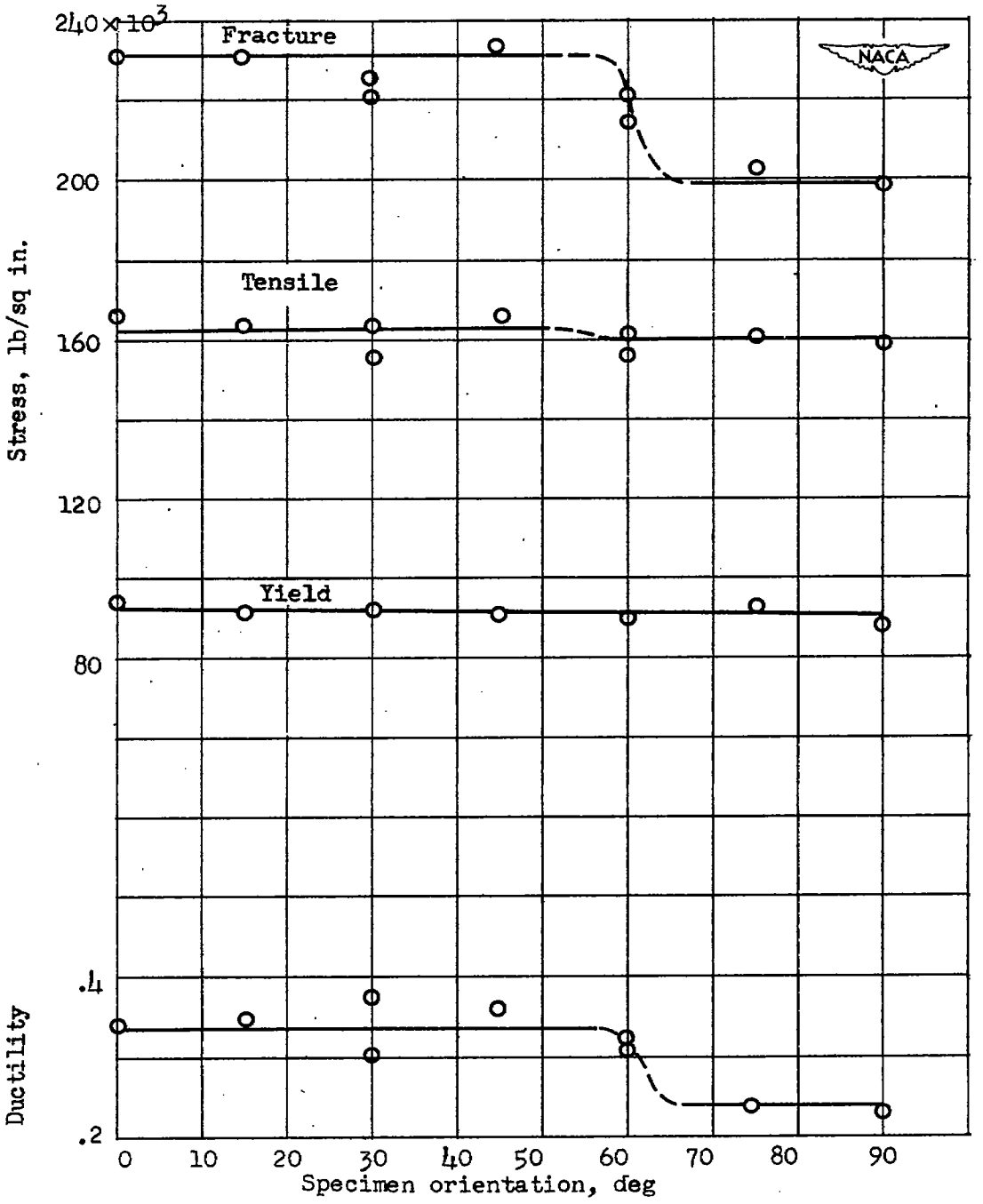

(c) Forged and heat-treated S-816.

Figure 6. - Concluded. Variation of tensile properties with testing direction of several alloys.

2023

0° orientation 90° orientation

(a) 16-25-6 electrolytically etched with 5-percent oxalic acid.

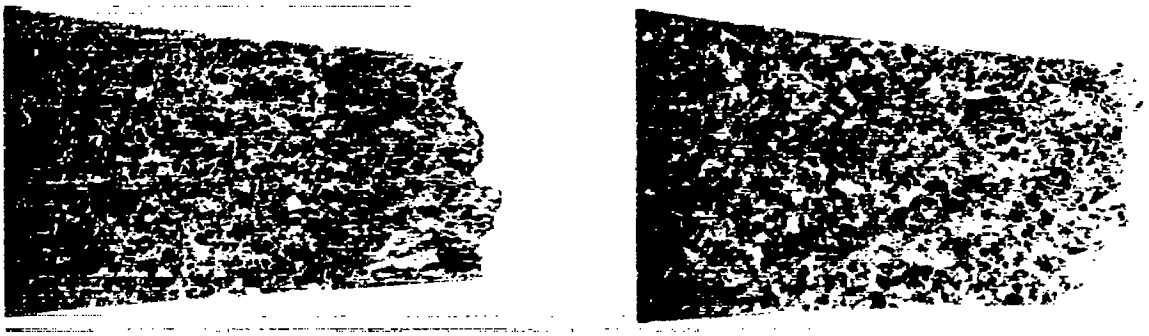

0° orientation 90° orientation

(b) Inconel X etched with aqua regia plus cupric chloride.

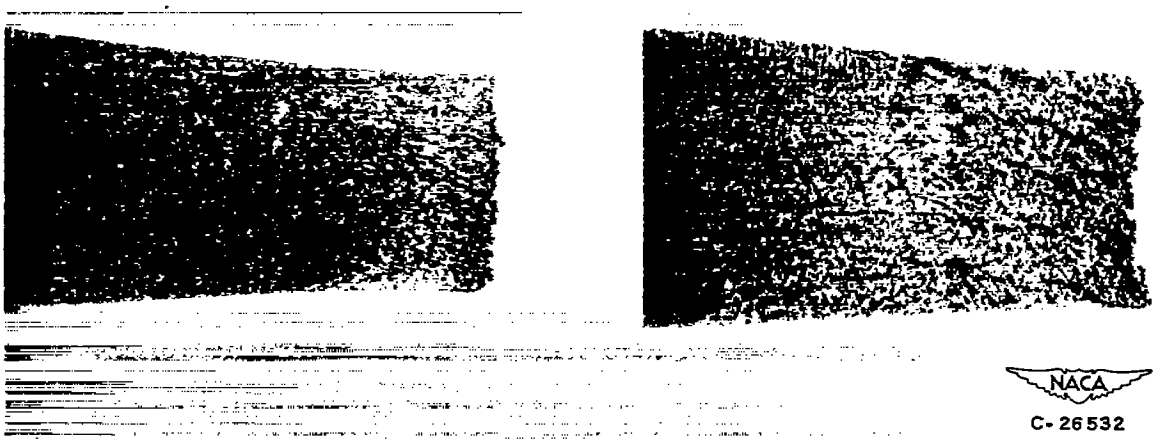

0° orientation 90° orientation

(c) S-816 etched with alcohol plus aqua regia.

Figure 7. - Longitudinal sections of specimens having orientations of 0° and 90° for three alloys. X8.

(a) 45° orientation.

(b) 60° orientation.

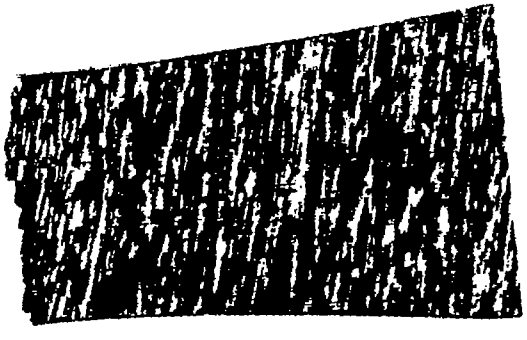

(c) 75° orientation.

NACA
C-26533

Figure 8. - Longitudinal sections of 16-25-6 specimens having various orientations. Electrolytically etched with 5-percent oxalic acid. X8.

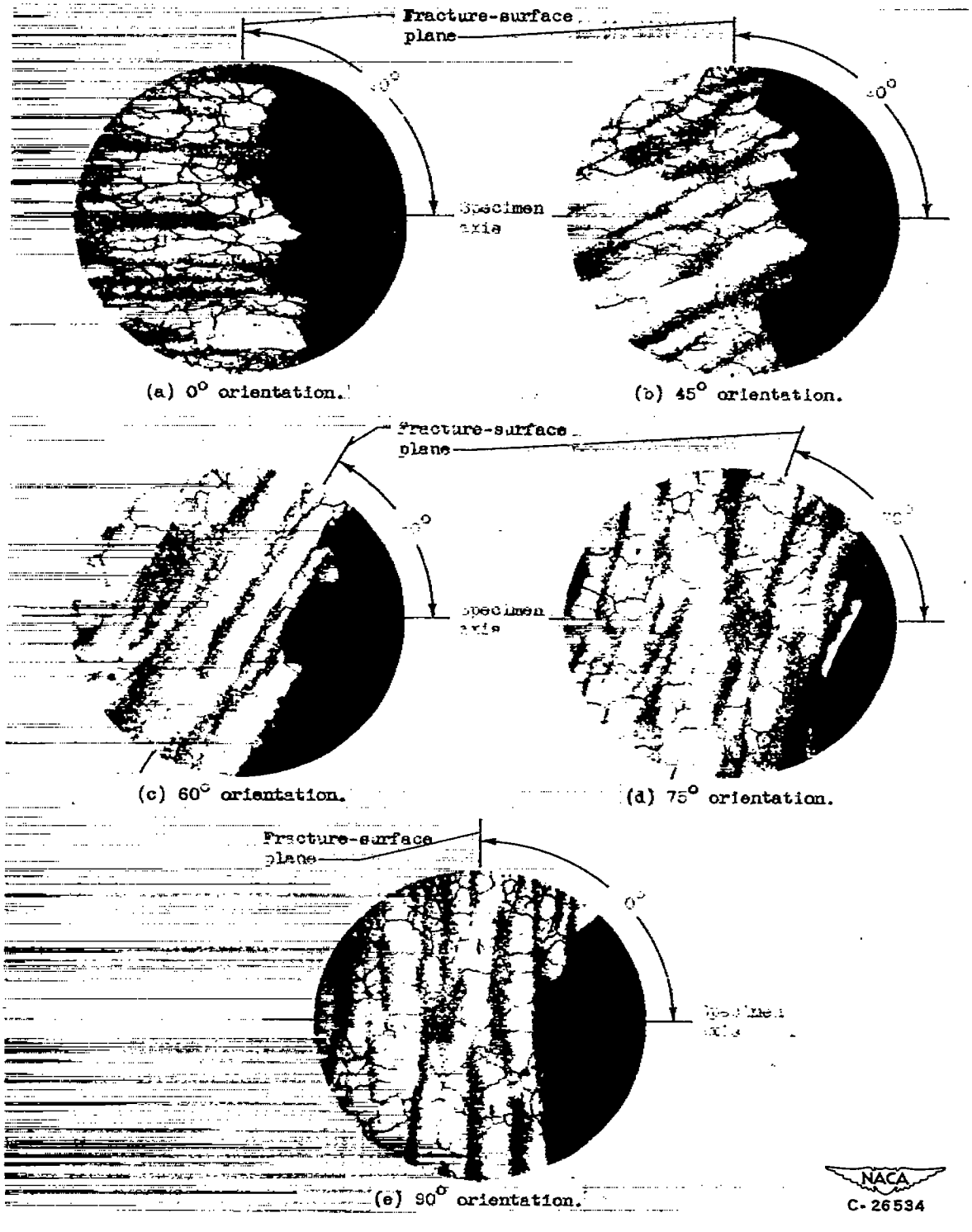

Figure 9. - Longitudinal sections of 16-25-6 specimens at fracture having various orientations. Electrolytically etched with 5-percent oxalic acid. X250.

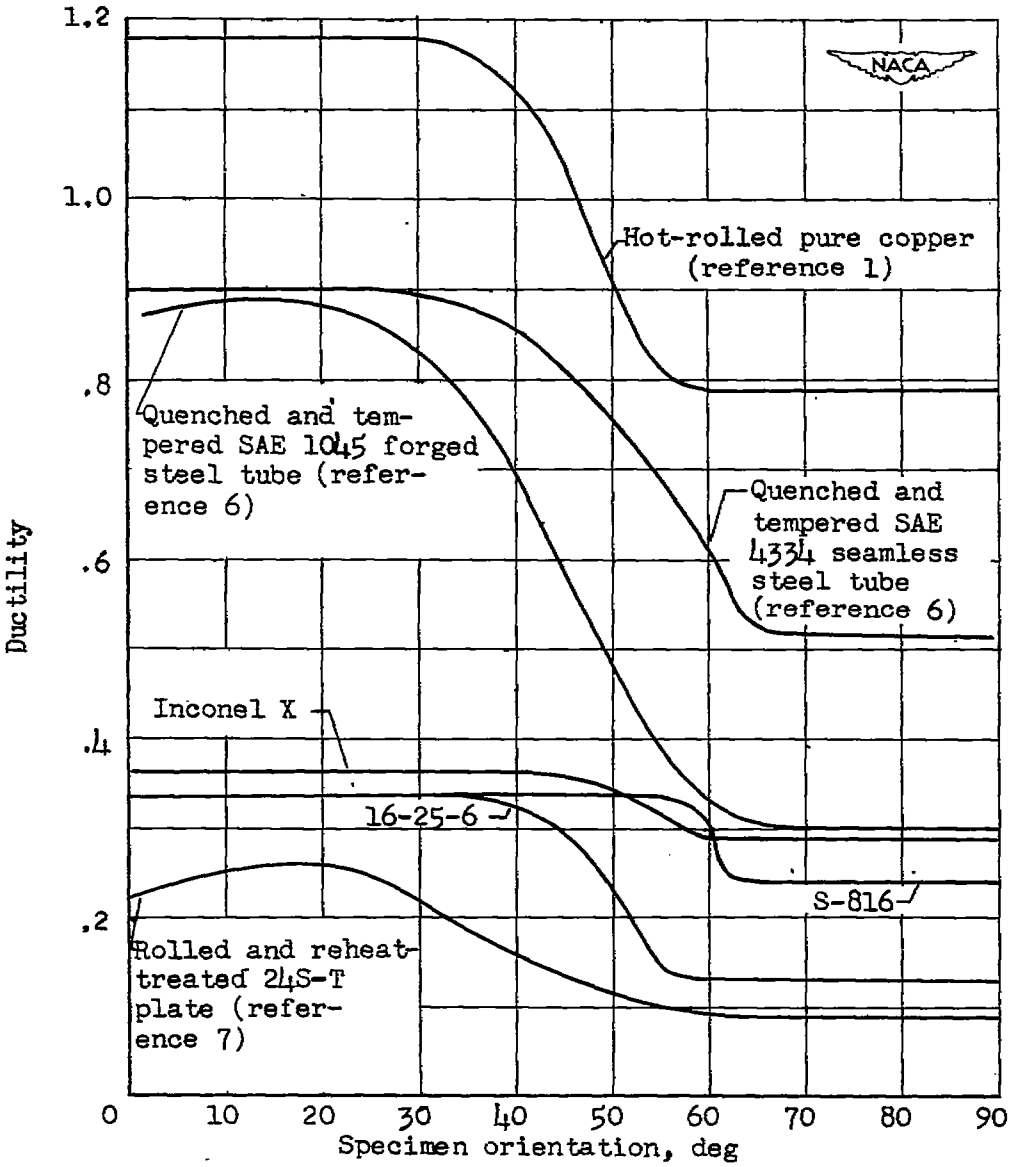

Figure 10. - Variation in ductility with testing direction for various materials.

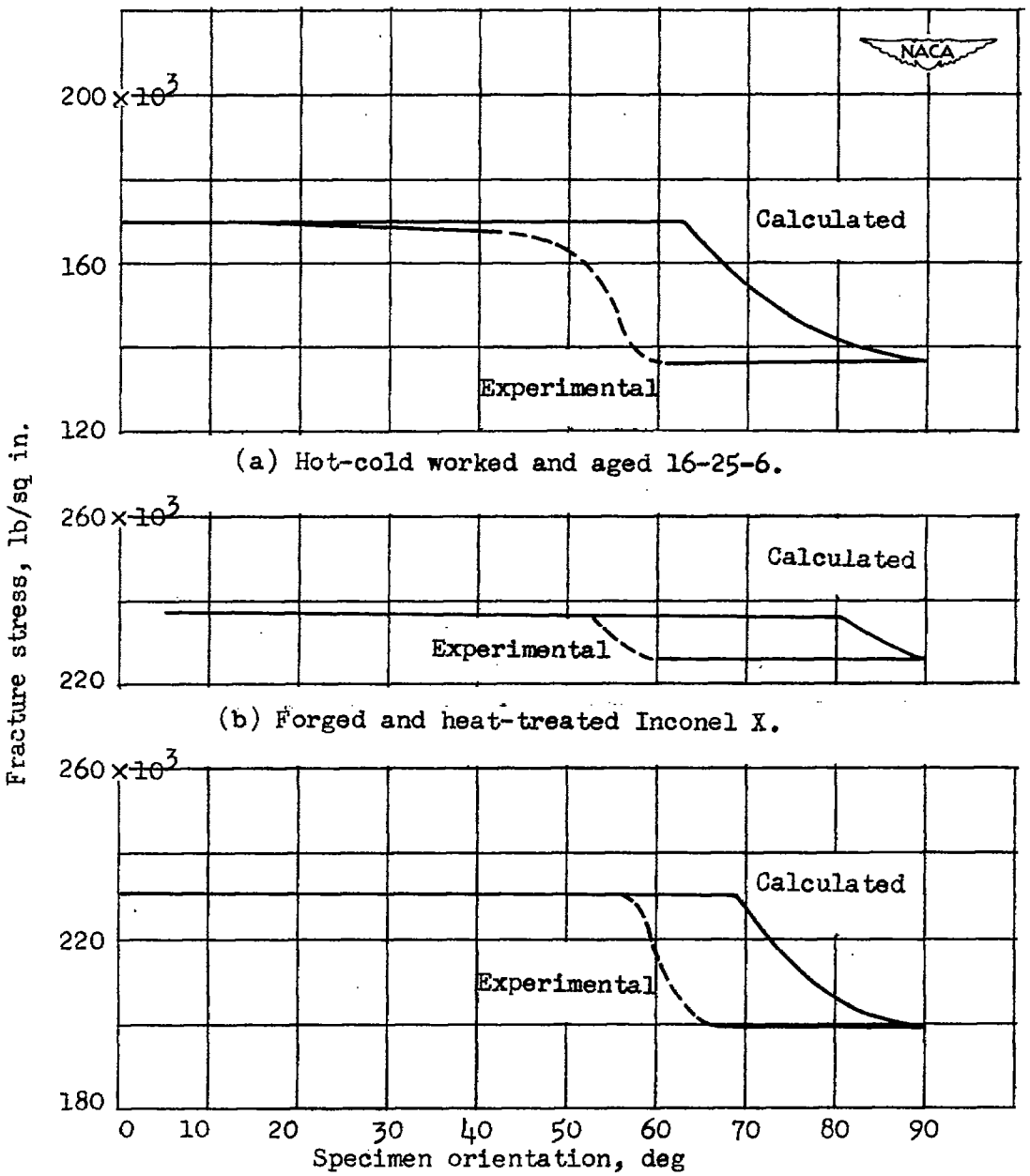

(c) Forged and heat-treated S-816.

Figure 11. - Comparison of calculated and experimental variation of fracture stress with testing direction for three alloys.

NASA Technical Library
3 1176 01435 2141